



## Microbial fuel cell as a biocapacitor by using pseudo-capacitive anode materials



Zhisheng Lv <sup>a,b</sup>, Daohai Xie <sup>a,b</sup>, Fusheng Li <sup>c</sup>, Yun Hu <sup>a,b</sup>, Chaohai Wei <sup>a,b</sup>, Chunhua Feng <sup>a,b,c,\*</sup>

<sup>a</sup> School of Environment and Energy, South China University of Technology, Guangzhou 510006, PR China

<sup>b</sup> The Key Lab of Pollution Control and Ecosystem Restoration in Industry Clusters, Ministry of Education, School of Environmental Science and Engineering, South China University of Technology, Guangzhou 510006, PR China

<sup>c</sup> River Basin Research Center, Gifu University, 1-1 Yanagido, Gifu City 501-1193, Japan

### HIGHLIGHTS

- Microbial fuel cell as a biocapacitor by using pseudo-capacitive anode materials.
- The biocapacitor stores electrons generated from microbial oxidation of substrate.
- The average power significantly increases if the stored energy is shortly dissipated.
- The charge/energy stored and released is highly dependent on the anode capacitance.

### ARTICLE INFO

#### Article history:

Received 15 May 2013

Received in revised form

12 July 2013

Accepted 4 August 2013

Available online 15 August 2013

#### Keywords:

Microbial fuel cell

Biocapacitor

Biocapacitive anode

Ruthenium oxide

Conducting polymer

### ABSTRACT

Here, we report that the microbial fuel cell (MFC) containing pseudo-capacitive anode materials such as polypyrrole (PPy)/9,10-anthraquinone-2-sulfonic acid sodium salt (AQS) composite films and RuO<sub>2</sub> nanoparticles can function as a biocapacitor, able to store bioelectrons generated from microbial oxidation of substrate and release the accumulated charge upon requirement. Influences of the specific capacitance of the PPy/AQS- and RuO<sub>2</sub>-modified carbon felt anodes on the extent of accumulated charge are examined. Results show that increasing anode capacitance is responsible for the increases in the amount of electrons stored and released, and thereby leading to more energy stored and average power dissipated. The long-term charging–discharging tests indicate that the RuO<sub>2</sub>-modified biocapacitor with a specific capacitance of 3.74 F cm<sup>-2</sup> exhibits 6% loss in the amount of released charge over 10 cycles for one-month operation, and 40% loss over 60 cycles for six-month operation. Our findings suggest that the MFC anode incorporating pseudo-capacitive materials shows potential for storing energy from waste organic matter and releasing in a short time of high power to the electronic device.

© 2013 Elsevier B.V. All rights reserved.

## 1. Introduction

Microbial fuel cells (MFCs) are attractive for environmental-friendly sustainable power applications, because they are able to produce electricity by oxidizing a variety of organic substrates available in wastewaters with microorganisms. Due to the sluggish anode kinetics and the limited organic concentrations in wastewaters, the power generated from MFCs is orders of magnitude smaller than that associated with hydrogen-based fuel cells [1,2].

Many of the studies to date have concentrated on improving anode performance by the search of effective anode materials [3–8] and microorganisms [9,10] in order to boost the power. However, the resulting power was still limited with respect to the power demand of most electronic devices [11,12]. To fill the gap, some researchers [11,13,14] have proposed an alternative solution by which the energy generated in MFCs are first accumulated in an external capacitor and then dissipated in a short time of high power to the electronic device. Their results have shown that the use of capacitor allowed more energy harvested when MFCs were operated intermittently rather than continuously.

Instead of the use of the external capacitor, a recent study [15] has developed an integrated anode system that incorporated capacitive material into the bioanode, leading to the conclusion that the capacitive anode performed better than the noncapacitive

\* Corresponding author. School of Environment and Energy, South China University of Technology, Guangzhou 510006, PR China. Tel.: +86 20 39380502; fax: +86 20 39380588.

E-mail address: [chfeng@scut.edu.cn](mailto:chfeng@scut.edu.cn) (C. Feng).

counterpart in terms of more charge stored during the charge–discharge experiment. This novel concept makes the anode function as a biocapacitor which shares the same electrolyte, membrane and counter electrode (cathode) with the MFC. Thus, the MFC under such a case can not only generate bioelectricity, but also store and release energy. Fig. 1 illustrates the concept of using an MFC as the biocapacitor in which the anode accumulates electrons from bacteria for charging when switch is open and releases electrons to the external circuit for discharging when switch is closed.

Deeke and his coworkers [15] prepared the capacitive anode by adding activated carbon powder and polymers including NMP (*N*-methyl-2-pyrrolidone) and PVDF (poly(vinylidene fluoride)) to the current collector. However, these may not be the optimal anode materials due to their relatively low capacitance and low electrical conductivity. Indeed, pseudo-capacitive materials including transition metal oxides like RuO<sub>2</sub> and conductive polymers like polypyrrole (PPy) are more appropriate for being used in the anode owing to their fast and reversible redox behavior, large surface area, and favorable metallic conductivity [16,17]. It is well recognized that their capacitance is typically 2–3 times larger than that of the carbon based materials [18]. More importantly, our previous studies [19,20] have demonstrated that they can interact well with the microorganisms and promote electron transfer from the microorganisms to the anode. In particular, it is of great concern about how the anode capacitance affects the amounts of charge stored and how the long-term operation affects performance of the capacitive materials, because these are important considerations for selection of anode materials and optimization of experimental design.

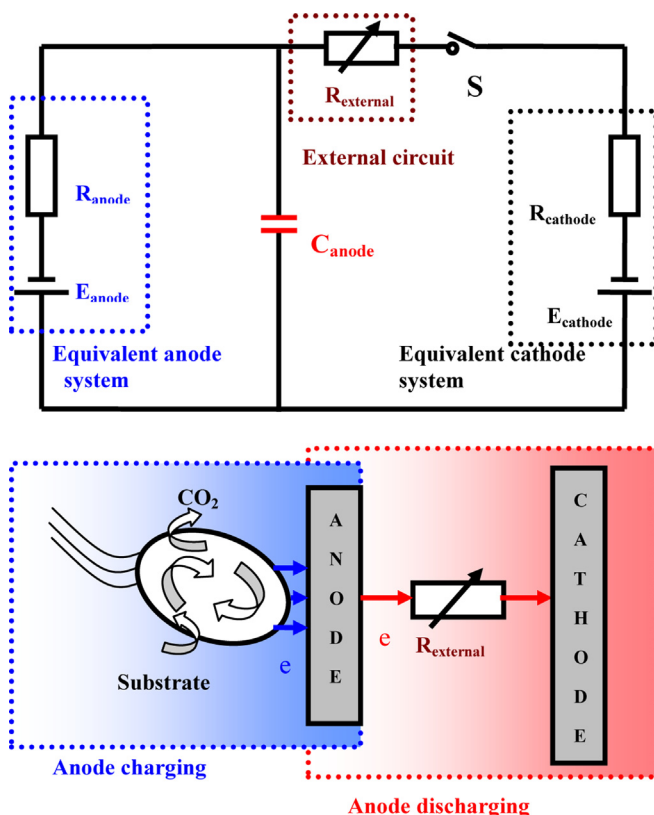


**Fig. 1.** Equivalent circuit of an MFC containing a capacitive anode. It consists of an equivalent anode system, an equivalent cathode system and an external circuit.  $R_{\text{anode}}$  and  $R_{\text{cathode}}$  represent the sum of charge-transfer resistance, diffusion resistance and ohmic resistance at the anode and cathode, respectively. The capacitive anode stores electrons from bacteria when switch S is open and releases electrons to the external circuit when switch S is closed.

The present study thus aimed to verify the ability of the anode containing pseudo-capacitive materials to function as a biocapacitor, which can store bioelectrons generated from microbial oxidation of substrate and release the accumulated charge during the discharge experiment. To meet this goal, a series of polypyrrole (PPy)/9,10-anthraquinone-2-sulfonic acid sodium salt (AQS)- and RuO<sub>2</sub>-modified carbon felt anodes were prepared and the influences of their specific capacitance on the extent of accumulated charge were evaluated. The energy stored in the biocapacitor was calculated and further calculation of the average power density was performed given that the energy was dissipated in a short time. In addition, attention was devoted to investigate the cycling durability of the biocapacitor by running the long-term tests with repeatable charging and discharging.

## 2. Experimental

### 2.1. Preparation of pseudo-capacitive anode materials

RuO<sub>2</sub> and conducting polymer are widely used in supercapacitor applications due to their electrical conductivity and reversible redox reactions. Here, PPy-modified and RuO<sub>2</sub>-modified carbon felt electrodes as the anodes were prepared according to the procedures described in our previous work [19,20]. The starting anode substrate was a piece of carbon felt (3.0 cm × 2.0 cm × 0.5 cm) that was cleaned in a hot H<sub>2</sub>O<sub>2</sub> (10%, 90 °C) solution for 3 h, followed by thorough rinse with deionized water and dry at 60 °C. A Ti wire (1 mm in diameter) was inserted inside the carbon felt to allow the external circuit connection. The room-temperature electrodeposition was performed in a three-electrode electrochemical cell including a working electrode (carbon felt), a reference electrode (saturated calomel electrode, SCE) and a counter electrode (Pt mesh). It should be noted that all the potentials reported throughout this paper were referred to SCE, if not otherwise stated. To deposit AQS doped-PPy films on the carbon felt, a constant potential of 0.8 V was applied for the anodic electropolymerization in a non-stirred N<sub>2</sub>-saturated solution that contained 0.1 M pyrrole monomer and 5 mM AQS. RuO<sub>2</sub>-modified carbon felt samples were prepared from a RuCl<sub>3</sub> (0.05 M) solution under the galvanostatic condition by applying a constant current density of 5 mA cm<sup>-2</sup> (normalized to the projected area of electrode) which was controlled by a potentiostat (CHI 660C, Shanghai CH Instrument Company, China). The difference in capacitance among these modifying materials was controlled by varying the total charge passed to the working electrode. The freshly prepared RuO<sub>2</sub>-modified and PPy/AQS-modified carbon felt anodes were then thoroughly rinsed with distilled water and air-dried at room temperature.

The capacitance of the synthesized materials was examined through the galvanostatic charge–discharge tests that were performed at a current load of 0.5 mA cm<sup>-2</sup> within the potential window from −0.6 to 0.3 V. The EIS measurements on resistance of the anode materials were performed by recording the impedance spectra at the open circuit potential (OCP) and in the frequency range from 10,000 to 0.01 Hz with a sinusoidal excitation signal of 10 mV. All these electrochemical tests were carried out in 0.1 M Na<sub>2</sub>SO<sub>4</sub> solution using the same three-electrode electrochemical cell as described above.

### 2.2. MFC construction, operation and tests

The two-chamber MFC made of Perspex flames was fabricated as described previously [19–21], consisting of the modified carbon felt anode and a bare carbon felt cathode (3.0 cm × 2.0 cm × 0.5 cm) in each chamber. The two chambers were separated by a cation exchange membrane (Zhejiang Qianqi Group Co., Ltd. China) with

each having an effective volume of 25 mL. The anode chamber was inoculated with *Shewanella oneidensis* MR-1 purchased from ATCC (700550). The anolyte contained the lactate-growth medium including 20 mM lactate and 0.1 M phosphate buffer solution (PBS)-based nutrient solution (pH 8.0) consisting of 5.84 g L<sup>-1</sup> NaCl, 0.10 g L<sup>-1</sup> KCl, 0.25 g L<sup>-1</sup> NH<sub>4</sub>Cl, 10 mL of vitamin solution and 10 mL of mineral solution. The cathode chamber was fed with a PBS solution (0.1 M, pH 7.0) containing 50 mM potassium hexacyanoferrate as the electron acceptor. All MFCs were operated at a controlled temperature of 30 °C. A 32-channel voltage collection instrument (AD8223, China) was used to record the cell voltages with a 2000 Ω external resistance.

### 2.3. Charging and discharging tests

When the MFC was run at a steady state which was indicated by a relatively constant cell voltage output with an external resistance of 2000 Ω, the external circuit was open. Under such a case, anode charging occurs because the electrons released from the microbial oxidation of lactate can be stored in the anode, as illustrated in Fig. 1. The anodes were considered to be fully charged when the anode potentials decreased to the open-circuit value. The charging time was varied from 2 to 5 h, depending on the anode capacitance. The discharging tests were performed with chronoamperometry at a polarization potential of 0 V in a three-electrode mode. The anode, the SCE in the anode chamber and the cathode was used as the working electrode, the reference electrode and the counter electrode, respectively. The discharging time was 20 min.

For the long-term experiments, the biocapacitor (i.e., MFC) was operated over six months and repeatedly amended with the fresh substrate once it was consumed by microbial oxidation. The charging and discharging tests were performed during each feeding cycle, following the procedure described above.

### 2.4. Scanning electron microscope (SEM) tests

Surface morphologies of the anodes before and after inoculation with bacteria were examined using SEM (S-3000N or S-3700N, Hitachi, Japan). To stabilize the bacteria attached to the anode, the sample (cut from the anode) was first immersed in 3% glutaraldehyde solution for 5 h. It was then rinsed with a PBS solution (pH 7.0) three times, followed by dehydration with increasing concentration of ethanol (34%, 50%, 75%, and 95%) for 10 min each and further rinses in isoamyl acetate twice (10 min each time). Prior to SEM tests, the sample was dried at CO<sub>2</sub>-critical point for 3 h and then sputtered with a thin coating layer of gold.

## 3. Results and discussion

### 3.1. Specific capacitance of pseudo-capacitive anode materials

A series of anode materials consisting of PPy/AQS or RuO<sub>2</sub> composite films modified on the carbon felt electrodes were prepared by electrodeposition and their capacitances were determined before they were mounted onto the anodes of MFCs. Scanning electron microscopy (SEM) tests showed that all of them possessed a submicron-/nano-composite network structure (data not shown), as illustrated in our previous reports [20,22]. Changes in the specific capacitance as a function of the controlled charges applied for electrodeposition were investigated by galvanostatic tests. Fig. 2 shows that all the galvanostatic charging–discharging curves featured a mirror-like profile during one charge–discharge cycle, in good agreement with that observed in our previous work [22]. The high linearity and symmetry suggests that both PPy/AQS and RuO<sub>2</sub> exhibit

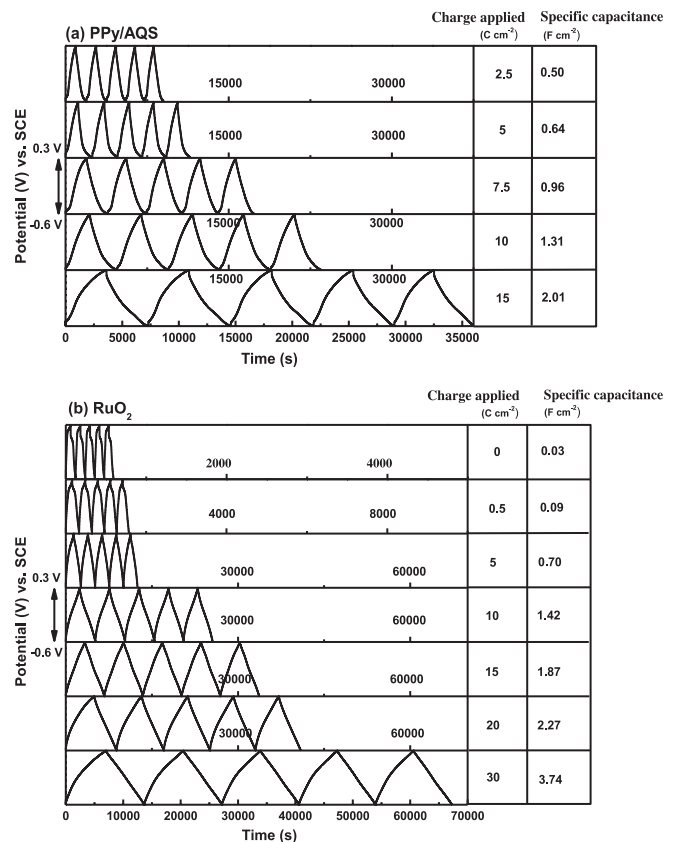


**Fig. 2.** Variations in galvanostatic charge–discharge curve as a result of different charge applied for the growth of PPy/AQS and RuO<sub>2</sub> composite films on the felt electrodes. Specific capacitance was calculated based on Equation (1). The control anode without modifications has a specific capacitance of 0.03 F cm<sup>-2</sup> corresponding to 0 C cm<sup>-2</sup> of applied charge.

good charging–discharging reversibility as capacitive materials. The specific capacitance (C) can be calculated from the curve according to:

$$C = \frac{I_{\text{charge-discharge}} \times t}{U_{\text{charge-discharge}} \times A} \quad (1)$$

where  $I_{\text{charge-discharge}}$  is the charge–discharge current;  $t$  is the discharge time;  $U_{\text{charge-discharge}}$  is the potential window; and  $A$  is the projected anode surface area. An increase in the specific capacitance with the increasing charge applied was clearly visible for all electrodes. For example, when the charge was changed from 0 to 15 C cm<sup>-2</sup>, the capacitance of PPy/AQS-modified electrode increased from 0.03 to 2.01 F cm<sup>-2</sup>. For RuO<sub>2</sub>-modified electrode, an applied charge of 30 C cm<sup>-2</sup> resulted in the capacitance of 3.74 F cm<sup>-2</sup>, increased by 2.6 times as compared to that associated with 10 C cm<sup>-2</sup> charge.

### 3.2. The modified anode functioning as a biocapacitor

To explore that the anodes modified with the pseudo-capacitive anode materials can function as capacitors, charging and discharging experiments were performed to identify their ability to store electrons from the bacteria under the open-circuit condition and release the accumulated charge upon a constant potential applied. For the charging tests, changes in the anode potential were recorded as a function of time after the electrical circuit was open. Fig. 3 shows the representative data collected from different anodes (including the unmodified carbon felt anode with a specific

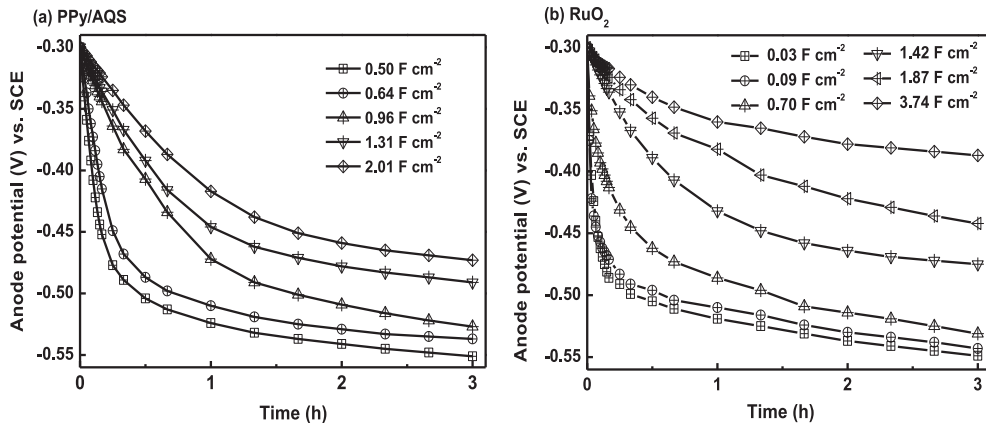


**Fig. 3.** Changes in anode potential for PPy/AQS- and RuO<sub>2</sub>-modified carbon felt anodes operated under the open-circuit condition. The potentials were recorded starting from the same anode potential of  $-0.30$  V. For comparison, data sets associated with the unmodified anode ( $0.03$  F cm $^{-2}$ ) were also shown.

capacitance of  $0.03$  F cm $^{-2}$ ) whose potentials decreased over time during the 3-h open-circuit operation. No immediate potential drop was observed for all the anodes. This observation was an indicative of the fact that the anodes had the ability to store electrons, otherwise the anode potential should drop to the open-circuit potential in a short time [15]. In addition, the extent of potential drop at the same time interval was strongly affected by the differences in the specific capacitance of the anode. As shown from Fig. 3, the 3-h open circuit operation caused a larger decrease in the potential from  $-0.30$  to  $-0.55$  V for the unmodified anode, as compared to the potential decrease from  $-0.30$  to  $-0.47$  V for the PPy/AQS-modified anode with the specific capacitance of  $2.01$  F cm $^{-2}$ . Increasing the specific capacitance of anodes either containing PPy/AQS or RuO<sub>2</sub>

decreased the rate of potential drop. The slowest potential decrease (from  $-0.30$  to  $-0.39$  V) corresponded well with the highest specific capacitance ( $3.74$  F cm $^{-2}$ ) of the investigated anodes.

After the anodes were fully charged as evident from the observation that these anode potentials decreased to the open-circuit value, they were allowed for discharge. Fig. 4a and b shows typical chronoamperometric curves obtained at a polarization potential of  $0$  V for different anodes (including the unmodified carbon felt anode with a specific capacitance of  $0.03$  F cm $^{-2}$ ) that were charged under the open-circuit condition. All the curves exhibited a current peak at the beginning of the discharge test, followed by a rapid current decay until it approached a relatively constant value. This profile was in consistent with the previous study [23] showing

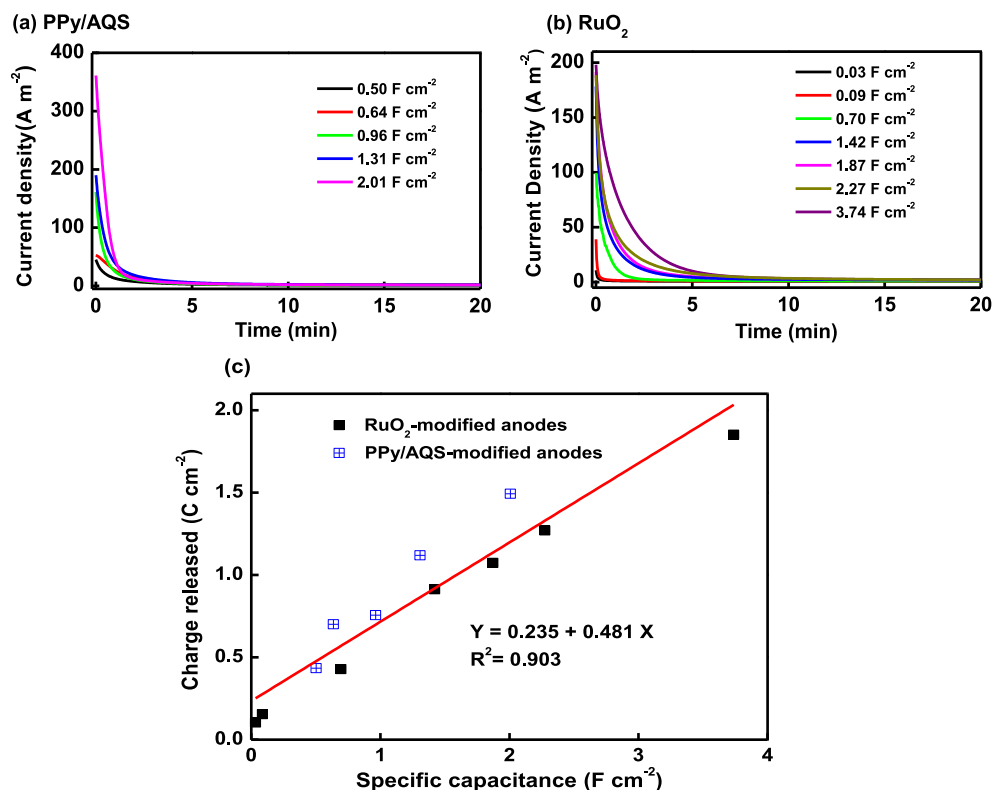


**Fig. 4.** Chronoamperometric curves polarized at  $0$  V for (a) PPy/AQS- and (b) RuO<sub>2</sub>-modified carbon felt anodes that were charged by the bioelectrons under the open-circuit condition. For comparison, data sets associated with the unmodified anode ( $0.03$  F cm $^{-2}$ ) were also shown. (c) Correlation of the amount of charge released with the specific capacitance of anode. The best-fit linear correlation is shown by the solid line. (Color version of this figure is available online.)

that the capacitive anode had the ability to store electrons. The height of the peak was found to highly depend on the specific capacitance. By integrating the discharge current ( $I$ ) with the time ( $t$ ), the accumulated charge ( $Q$ ) released during chronoamperometric tests was obtained, as illustrated in the following equation:

$$Q = \int_0^t Idt \quad (2)$$

It has been shown in Fig. 4c that for PPy/AQS- or RuO<sub>2</sub>-modified carbon felt anodes, the larger the specific capacitance, the greater the amount of charge released. For example, the RuO<sub>2</sub>-modified anode with a capacitance of 3.74 F cm<sup>-2</sup> can release 1.85 C cm<sup>-2</sup> of charge, 18 times larger than 0.10 C cm<sup>-2</sup> associated with the unmodified anode. A linear relationship between them was observed as indicated by  $R^2 = 0.903$  for regression of all of the anodes together.

The data presented in Figs. 3 and 4 provided evidence that the anode having high capacitance was able to function as a biocapacitor and that the increasing anode capacitance was responsible for

more electrons stored and then released. Several previous studies [23–26] have reported the promising findings that c-type cytochromes embedded in the biofilms can act as capacitors to store electrons in the periplasm and outer membrane, opening new possibilities for design of supercapacitor using living microbes [27]. It is likely that the amount of charge stored under the open-circuit condition does not only depend on the pseudo-capacitance materials but also on the biofilms.

To identify the contribution of the biofilm capacitance to the overall capacitance of the modified anode with bacteria, the unmodified anode with the lowest value of capacitance (0.03 F cm<sup>-2</sup>) was chosen for this investigation because it is relatively stable upon long-term tests and its capacitance may not obscure the contribution of biofilm capacitance. Fig. 5a–d shows the SEM images of biofilm grown on the unmodified carbon felt anode. It was noticeable that increasing operation time resulted in a drastic increase in the amount of bacteria attached on the solid electrode. Fig. 5e presents the galvanostatic charge–discharge curves of this anode recorded at Day 0 (without bacteria), Day 14 and Day 180,

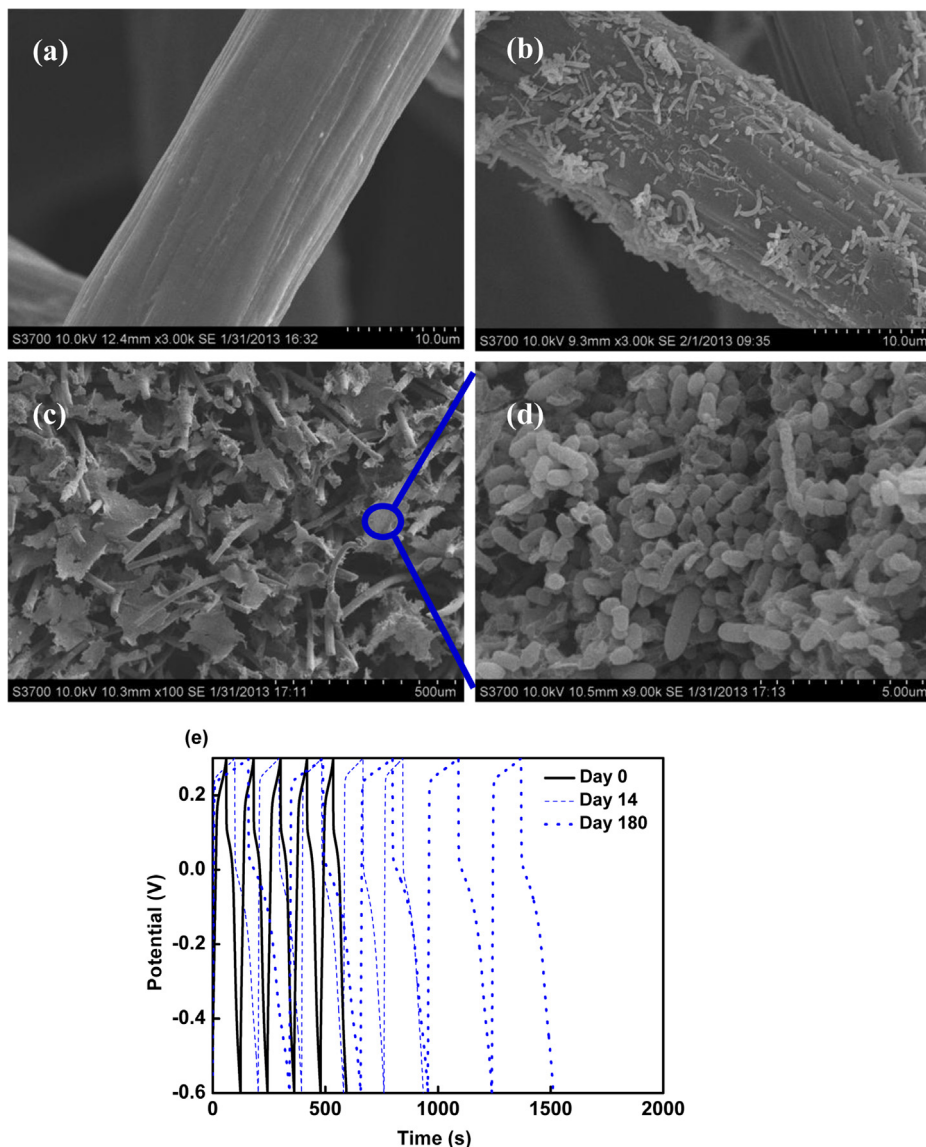


**Fig. 5.** SEM images of the unmodified carbon felt anode taken (a) at Day 0 without the inoculation of *Shewanella oneidensis* MR-1, (b) at Day 14 and (c & d) Day 180 with the inoculation of *Shewanella oneidensis* MR-1, with magnification of (a) 3000 $\times$ , (b) 3000 $\times$ , (c) 100 $\times$  and (d) 9000 $\times$ . (d) Galvanostatic charge–discharge curves of the unmodified anode recorded at Day 0 (without bacteria), Day 14 and Day 180.

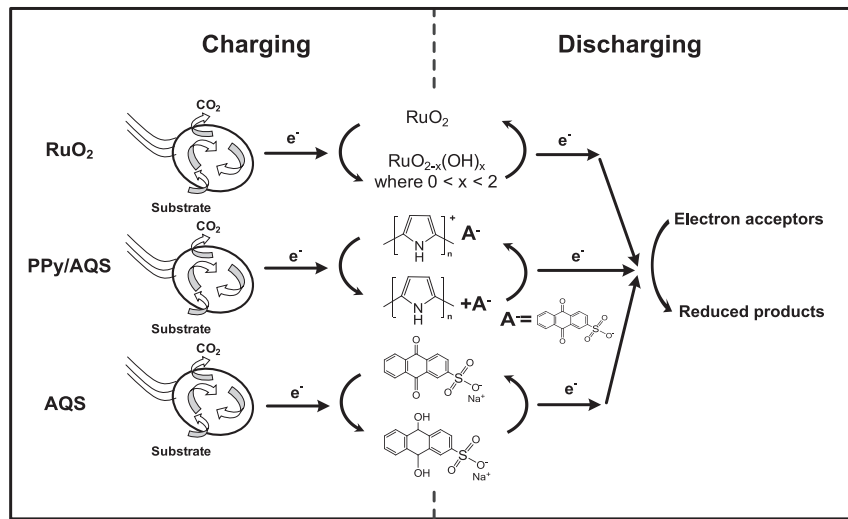


Fig. 6. Mechanism governing electron transport in the biocapacitor equipped with RuO<sub>2</sub>-modified or PPy/AQS-modified carbon felt anode.

indicating the increased capacitance due to more amounts of bacteria grown. The calculated anode capacitance was 0.03, 0.05, and 0.08 F cm<sup>-2</sup>, corresponding to Day 0, Day 14 and Day 180, respectively. The difference in the anode capacitance between the bacteria-adhered anode and the abiotic control was considered to be the *Shewanella* biofilm capacitance, by assuming that long-term tests caused insignificant loss of capacitance associated with the substrate material (i.e., carbon felt). It was found that operation of 14 days resulted in a biofilm capacitance of 0.02 F cm<sup>-2</sup>. Despite the distinct observation of thick biofilm grown on the carbon felt anode over 180-day operation, the anode at Day 180 exhibited a biofilm capacitance of 0.05 F cm<sup>-2</sup> that was only 2.5 times larger than that obtained at Day 14. This should be ascribed to the low electrical conductivity of bacteria, an intrinsic feature of living organisms.

It should be noted that the capacitance value of 0.05 F cm<sup>-2</sup> in relation to *Shewanella* biofilm is much larger than that (0.62 mF cm<sup>-2</sup>) of *Geobacter* biofilm as reported by Malvankar et al. [27], possibly due to the facts that *G. sulfurreducens* biofilms were grown on a gold electrode which has a much smaller specific surface area, and that the duration time for acclimation of *Geobacter* biofilm was only 100 h. Our reported value is comparative to that associated with mixed microbial culture grown on the activated carbon anode [28]. Nevertheless, the value (0.05 F cm<sup>-2</sup>) at Day 180 was still 10–75 times lower than that of synthesized capacitive materials, confirming that the contribution of the *Shewanella* biofilm grown on the modified electrodes to the overall anode capacitance was insignificant, particularly in regards to the RuO<sub>2</sub>-modified anode with a capacitance of 3.74 F cm<sup>-2</sup>.

### 3.3. Electron transport mechanism in the biocapacitor

The mechanism governing electron transport in the biocapacitor is proposed and illustrated in Fig. 6. Here, possible reactions involved for charging and discharging were presented. Under the case of anode charging, biotic and abiotic reactions take place sequentially. Microbial oxidation of organic substrate first generates bioelectrons which are then transferred to the solid anode surface. For the RuO<sub>2</sub>-modified carbon felt anode, these electrons drive the reduction reactions between the oxidation states Ru (IV) and Ru (II); For the PPy/AQS-modified carbon felt anode, both PPy and AQS can react with the electrons, resulting in the formation of reduced PPy and AQS. In comparison to microbial reaction of liberated electrons from organic substrate, the abiotic reactions

proceed at a faster rate. Under the case of anode discharging, the stored electrons are then released as a consequence of the re-oxidation of Ru (II) or reduced PPy and AQS, coupled to the reduction of the terminal electron acceptors.

### 3.4. Calculations on the energy stored in the biocapacitor and average power density dissipated in a short time

The energy (W) stored in the biocapacitor during the open-circuit charging was calculated based on the following equation:

$$W = \frac{1}{2} CU^2 \quad (3)$$

where C is the specific capacitance of anode; U is the anode potential after charging. If the energy was dissipated in a short time (t), the average power generation (P) can be expressed as:

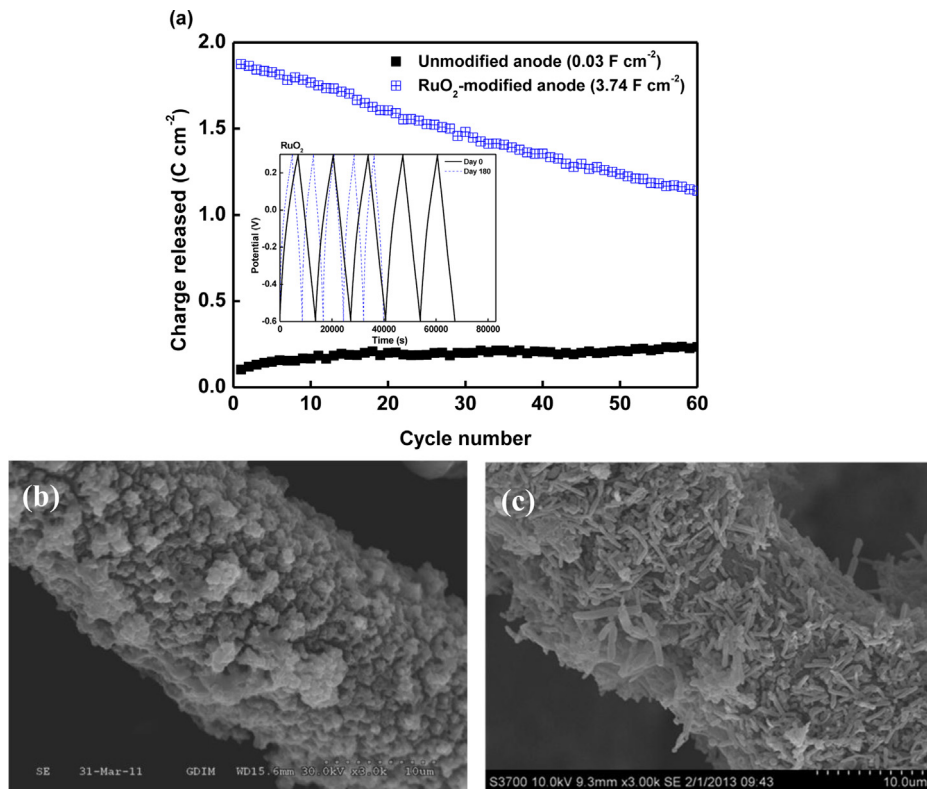
$$P = \frac{W}{t} \quad (4)$$

Table 1 lists the values of the energy and average power density as a function of the anode capacitance. The results indicated that

Table 1

Dependence of stored energy and average power density on anode capacitance. Average power density was calculated assuming the stored energy was dissipated in a short time.

Surface modifications	Specific capacitance (F cm <sup>-2</sup> )	Specific Energy stored (W h m <sup>-2</sup> )	Average power density (W m <sup>-2</sup> ) calculated based on the stored energy dissipated in a specific time (t)	
			t = 1 min	t = 10 min
Unmodified carbon felt anode	0.03	0.013	0.80	0.080
PPy/AQS-modified carbon felt anodes	0.50	0.22	12.98	1.30
	0.64	0.27	16.35	1.64
	0.96	0.41	24.45	2.45
	1.31	0.55	32.71	3.27
	2.01	0.81	48.79	4.88
RuO <sub>2</sub> -modified carbon felt anodes	0.09	0.036	2.14	0.21
	0.70	0.47	27.98	2.798
	1.42	0.58	34.55	3.46
	1.87	0.71	42.34	4.23
	3.74	1.19	71.43	7.14



**Fig. 7.** (a) Comparison of durability as a function of cycle number between the biocapacitor with the RuO<sub>2</sub>-modified anode (3.74 F cm<sup>-2</sup>) and the control biocapacitor with the unmodified anode. The inset figure shows the galvanostatic charge–discharge curves of the RuO<sub>2</sub>-modified anode recorded at Day 0 and Day 180, respectively. SEM images of the RuO<sub>2</sub>-modified carbon felt anode taken at (b) Day 0 without the inoculation of *Shewanella oneidensis* MR-1, and (c) Day 180 with the inoculation of *Shewanella oneidensis* MR-1.

the energy stored and the average power generation was strongly dependent on the anode capacitance, in agreement with the relationship between the amount of released charge with the anode capacitance. Also, it can be seen that the 1-min discharge of the stored energy for the RuO<sub>2</sub>-biocapacitor (3.74 F cm<sup>-2</sup>) resulted in an average power density of 71.43 W m<sup>-2</sup>, while this value largely decreased with the increase in the discharge time, with 7.14 W m<sup>-2</sup> related to the 10-min discharge. These values were much higher than those (e.g., 0.1–4 W m<sup>-2</sup>) reported in the current studies [29–34] among which the MFC was operated continuously. These results suggested that the biocapacitor, operated in an intermittent mode, has potential of powering some electronic devices.

### 3.5. Cycling durability of the biocapacitor

The cycling durability of the biocapacitor was evaluated by running the long-term tests with repeatable charging–discharging experiments. Fig. 7a shows the representative data with respect to the RuO<sub>2</sub> biocapacitor and the control biocapacitor. For the RuO<sub>2</sub>-modified anode with an initial capacitance of 3.74 F cm<sup>-2</sup>, it can be seen that 10-cycle operation (about one month) caused 6% loss in the released charge, whereas 40% loss was observed for 60 cycles (about six months). In contrast, for the unmodified carbon felt anode with an initial capacitance of 0.03 F cm<sup>-2</sup>, the released charge after the six-month operation increased by a factor of 2.4 as compared to the value obtained in the first cycle. The loss or increase is mainly attributed to the decrease or increase in the capacitance of the used anode, as evident from Figs. 5d and 7a. For example, the used RuO<sub>2</sub>-modified anode possessed a specific capacitance of 2.22 F cm<sup>-2</sup>, decreased by 41% compared to its initial

value. By fitting 2.22 F cm<sup>-2</sup> with the linear regression equation (Fig. 4c), one can predict the charge value of 1.30 C cm<sup>-2</sup>, which was approximately equal to 1.13 C cm<sup>-2</sup> measured after 60-cycle operation.

Although the long-term operation allowed the growth of thick biofilm (Fig. 7c and d) that contributed to the overall anode capacitance, the dissolution of the modifying materials upon repeatable charging and discharging should account for the remarkable decrease in the capacitance of the RuO<sub>2</sub>-modified anode. This is evident also from the SEM results (Fig. 7c and d) that the three-dimension RuO<sub>2</sub> particles visible in the electrode surface at Day 0 distinctly disappeared from the electrode surface at Day 180. Since the biocapacitor with pseudo-capacitive materials like RuO<sub>2</sub> involve chemical reactions of the electrode usually with phase change, some of the materials may be corroded by both biotic or abiotic processes and loss slowly through dissolving as a form of ion into the anodic electrolyte. Although these chemical reactions are relatively reversible, the repeatable charging and discharging tests often result in irreversible reaction products. In addition, the strain developed in the pure metal oxide during the charging and discharging tests causes the cracking of the electrode, leading to the dissolution of solid particles after long-term operation [35]. To address this issue, further research is suggested to construct anodes with hybrid composites consisting of pseudo-capacitive materials and non-electrochemical capacitive materials (e.g., carbon-base materials). The latter materials usually exhibit better cyclic stability since the electrode undergoes no chemical change during the charging and discharging process but have lower capacitance as compared to the pseudo-capacitive materials [16]. It is expected that the hybrid composites combine the merits and mitigate the shortcomings of both materials.

## 4. Conclusions

The major problem for real applications of MFC as a clean power source is the much lower amount of power generated than that required by most electronic devices, emphasizing the need to develop new strategy for filling the gap. Use of a capacitor to store energy produced by MFC proves to be an effective approach [11,13,14], because it enables energy delivery in short bursts to satisfy the power requirements. Here, we demonstrated that integration of high-capacitance pseudo-capacitive material into the anode has successfully made MFC function as a biocapacitor, able to store electrons produced from microbial oxidation of organic substrate under the open-circuit condition and release these electrons in a short time of enhanced power. The specific capacitance of anode is an important factor controlling the amount of energy stored and further influencing the power generation once the stored energy was dissipated in a short time. Results showed a linear relationship between the anode capacitance with the amount of charge accumulated and released. Long-term tests with repeatable charging–discharging measurements revealed that there was 40% loss in the capacity for charge storage with respect to the RuO<sub>2</sub>-modified biocapacitor operated over six months, mainly due to the decrease in the anode capacitance caused by the dissolution of the modifying materials.

## Acknowledgments

We gratefully acknowledge financial support from the National Natural Science Foundation of China (nos. 21177042 and 21037001), the Natural Science Foundation of Guangdong Province, China (no. S2011010002231), the Fundamental Research Funds for the Central Universities, SCUT (no. 2012ZZ0048) and the Program for New Century Excellent Talents in University (no. NCET-12-0198).

## References

- [1] A. Rinaldi, B. Mecheri, V. Garavaglia, S. Licoccia, P.D. Nardo, E. Traversa, *Energy Environ. Sci.* 1 (2008) 417–429.
- [2] T.H. Pham, P. Aelterman, W. Verstraete, *Trends Biotechnol.* 27 (2009) 168–178.
- [3] Y.J. Feng, Q. Yang, X. Wang, B.E. Logan, *J. Power Sources* 195 (2010) 1841–1844.
- [4] C. Li, L.B. Zhang, L.L. Ding, H.Q. Ren, H. Cui, *Biosens. Bioelectron.* 26 (2011) 4169–4176.
- [5] P. Luo, S.J. You, J.Y. Wang, *Biosens. Bioelectron.* 25 (2010) 1248–2151.
- [6] M. Sun, F. Zhang, Z.H. Tong, G.P. Sheng, Y.Z. Chen, Y. Zhao, Y.P. Chen, S.Y. Zhou, G. Liu, Y.C. Tian, H.Q. Yu, *Biosens. Bioelectron.* 26 (2010) 338–343.
- [7] L. Xiao, J. Damien, J.Y. Luo, H.D. Jang, J.X.Z. He, *J. Power Sources* 208 (2012) 187–192.
- [8] X.H. Peng, H.B. Yu, X. Wang, Q. Zhou, S.J. Zhang, L.J. Geng, J.W. Sun, Z. Cai, *Bioresour. Technol.* 121 (2012) 450–453.
- [9] H.J. Kim, H.S. Park, M.S. Hyun, I.S. Chang, M. Kim, B.H. Kim, *Enzym. Microb. Technol.* 30 (2002) 145–152.
- [10] N.T. Trinh, J.H. Park, B. Kim, *Korean J. Chem. Eng.* 26 (2009) 748–753.
- [11] A. Dewan, H. Beyenal, Z. Lewandowski, *Environ. Sci. Technol.* 43 (2009) 4600–4605.
- [12] Z.L. Wang, W.Z. Wu, *Angew. Chem. Int. Ed.* 51 (2012) 22–24.
- [13] Y. Kim, M.C. Hatzell, A.J. Hutchinson, B.E. Logan, *Energy Environ. Sci.* 4 (2011) 4662–4667.
- [14] P. Liang, W.L. Wu, J.C. Wei, L.L. Yuan, X. Xia, X. Huang, *Environ. Sci. Technol.* 45 (2011) 6647–6653.
- [15] A. Deekie, T.H.J.A. Sleutels, H.V.M. Hamelers, C.J.N. Buisman, *Environ. Sci. Technol.* 46 (2012) 3554–3560.
- [16] L.L. Zhang, X.S. Zhao, *Chem. Soc. Rev.* 38 (2009) 2520–2531.
- [17] P. Simon, Y. Gogotsi, *Nat. Mater.* 7 (2008) 845–854.
- [18] J. Jiang, Y.Y. Li, J.P. Liu, X.T. Huang, C.Z. Yuan, X.W. (David) Lou, *Adv. Mater.* 24 (2012) 5166–5180.
- [19] C.H. Feng, L. Ma, F.B. Li, H.J. Mai, X.M. Lang, S.S. Fan, *Biosens. Bioelectron.* 25 (2010) 1516–1520.
- [20] Z.S. Lv, D.H. Xie, X.J. Yue, C.H. Feng, C.H. Wei, *J. Power Source* 210 (2012) 26–31.
- [21] C.H. Feng, F.B. Li, H.Y. Liu, X.M. Lang, S.S. Fan, *Electrochim. Acta* 55 (2010) 2048–2054.
- [22] X.M. Lang, Q.Y. Wan, C.H. Feng, X.J. Yue, W.D. Xu, J. Li, S.S. Fan, *Synth. Met.* 160 (2010) 1800–1804.
- [23] N. Uría, X.M. Berbel, Olga Sánchez, F.X. Muñoz, J. Mas, *Environ. Sci. Technol.* 45 (2011) 10250–10256.
- [24] A. Esteve-Núñez, J. Sosnik, P. Visconti, D.R. Loveley, *Environ. Microbiol.* 10 (2008) 497–505.
- [25] P.S. Bonanmi, G.D. Schrott, L. Robuschi, J.P. Busalmen, *Energy Environ. Sci.* 5 (2012) 6188–6195.
- [26] G.D. Schrott, P.S. Bonanni, L. Robuschi, A. Esteve-Núñez, J.P. Busalmen, *Electrochim. Acta* 56 (2011) 10791–10795.
- [27] N.S. Malvankar, T. Mester, M.T. Tuominen, D.R. Lovley, *ChemPhysChem* 13 (2012) 463–468.
- [28] X.H. Peng, H. Yu, H.B. Yu, X. Wang, *Bioresour. Technol.* 138 (2013) 353–358.
- [29] Z. He, S.D. Minteer, L.T. Angenent, *Environ. Sci. Technol.* 39 (2005) 5262–5267.
- [30] M.H. Osman, A.A. Shah, F.C. Walsh, *Biosens. Bioelectron.* 26 (2010) 953–963.
- [31] X. Wang, S.A. Cheng, Y.J. Feng, M.D. Merrill, T. Satio, B.E. Logan, *Environ. Sci. Technol.* 43 (2009) 6870–6874.
- [32] X. Xie, M. Ye, L.B. Hu, N. Liu, J.R. McDonough, W. Chen, H.N. Alshareef, C.S. Criddle, Y. Cui, *Energy Environ. Sci.* 5 (2012) 5265–5270.
- [33] Y.Z. Fan, S.K. Han, H. Liu, *Energy Environ. Sci.* 5 (2012) 8273–8280.
- [34] Y.F. Chen, Z.S. Lv, J.M. Xu, D.Q. Peng, Y.X. Liu, J.X. Chen, X.B. Sun, C.H. Feng, C.H. Wei, *J. Power Sources* 201 (2012) 136–141.
- [35] M.J. Zhi, C.C. Xiang, J.T. Li, N.Q. Wu, *Nanoscale* 5 (2013) 72–88.